Materials Letters 214 (2018) 276–279

Contents lists available at ScienceDirect

Materials Letters

journal homepage: www.elsevier.com/locate/mlblue

Improved ductility and toughness of an Al-Cu casting alloy by changing the geometrical morphology of dendritic grains

Qing-Long Zhao, Qing-Quan Zhang, Wei Zhang, Feng Qiu, Qi-Chuan Jiang *

Key Laboratory of Automobile Materials, Ministry of Education, and Department of Materials Science and Engineering, Jilin University, No. 5988 Renmin Street, Changchun 130025, PR China

ARTICLE INFO

Article history:
Received 21 October 2017
Received in revised form 6 December 2017
Accepted 8 December 2017
Available online 9 December 2017

Keywords:
Metals and alloys
Grain boundaries
Deformation and fracture
Microstructure

ABSTRACT

Different dendritic grain morphology of an Al-Cu alloy was obtained by adjusting the casting parameters. Compared to the equiaxed dendritic grains, the tortuous dendritic grains led to increased tensile elongation (from 10.4% to 16.8%) and work of fracture (from 11.2 J/mm^2 to 17.2 J/mm^2) by more than 50%, respectively. Meanwhile, the high tensile strength (~540 MPa) and grain size (~80 μm) were unchanged. The intergranular fracture crack zigzagged along tortuous grain boundaries, reducing the stress concentration at the crack tip and increasing the propagation resistance and path, leading to increased toughness and elongation. The zigzag morphology of grain boundaries was attributed to tortuous dendritic grains.

1. Introduction

Traditional high-strength aluminum casting alloys usually exhibit low ductility and toughness, which limits their application [1]. The fracture of aluminum casting alloys is usually initiated at coarse second-phase particles and grain boundaries, because of particle cracking or rupturing of eutectic matrix on grain boundaries [2,3]. Previous research mainly focused on the effect of grain size, second dendrite arm spacing and coarse particles on fracture, however, many efforts have been made to improve the ductility and toughness of aluminum casting alloy by grain refinement and heat treatment [4,5]. Meanwhile, limited research reported that tortuous grain boundary morphology influenced ductility-dip cracking during hot deformation and stress corrosion cracking in Ni alloys [6,7]. The change of dendritic grain morphology might also affect the ductility/toughness of cast aluminum alloys.

Cast Al-Cu alloys exhibited high strength, but its low ductility and toughness limit its application. In our previously studies, we found that a dendritic grain structure with medium grain size in Al-Cu exhibited higher elongation than the more refined grain structure, but its mechanism was unclear [8–10]. The present work reports a significant improvement in ductility and toughness of an Al-Cu casting alloy due to tortuous morphology of dendritic grains, retaining composition, grain size and mechanical strength unchanged. The microstructure and fracture behavior were experimentally investigated. The present work suggests a new approach of improving the ductility and toughness of cast alloys.

2. Experimental

The chemical composition of the Al-Cu alloy (in wt.%) was mainly Al-5Cu-0.45Mn (containing a small amount of other elements). 0.5 wt.% TiC nano-particles were added in the melt as grain refiner, and the casting procedure has been described in Ref. [9]. Two different molds were used to produce different grain morphology. The geometry of molds was illustrated in the Supplementary Material. T6 treatment was performed (12 h at 808 K and 10 h at 438 K). The tensile specimens were with a gauge length of 10 mm and a cross section of 5 mm × 2.5 mm. Tensile tests were performed by a servo-hydraulic material testing system (MTS 810) at room temperature with a strain rate of $3.0 \times 10^{-4}\ s^{-1}$. Three-point bend test was performed using an Instron materials testing machine (Instron 5689), and the sample size was 16 × 4 × 2 mm. A U-notch of 0.25 mm wide and 2 mm long was made in the middle of the longitudinal section. Every sample was polished before three-point bend testing. Fracture toughness parameters were calculated according to ref. [11]. The microstructure was observed by scanning electron microscopy (SEM, TESCAN VEGA 3) equipped with electron backscatter diffraction detector (EBSD). The EBSD data were analyzed by HKL Channel 5 software.

---

* Corresponding author.
E-mail address: jqc@jlu.edu.cn (Q.-C. Jiang).

https://doi.org/10.1016/j.matlet.2017.12.037
0167-577X/© 2017 Elsevier B.V. All rights reserved.

3. Results and discussion

Fig. 1(a) shows the mechanical strength of two samples was similar, as shown in Table 1. The total elongation of sample S2 was 16.8%, 1.6 times higher than that of sample S1 (10.4%). Fig.1 (b) shows that the peak load of sample S2 was similar to that of sample S1, but the load dropped more slowly in sample S2 than in S1 after the peak load. The linear-elastic plane-strain fracture toughness of sample S1 and S2 was similar (Table 1), but the elastic-plastic plane-strain fracture toughness and work of fracture of sample S2 were 14.3% and 56% higher than those of sample S1, respectively.

Fig. 2(a–b) indicates that both of samples S1 and S2 showed intergranular fracture. The macro-crack in three-point bent sample S1 was relatively straight and sharp, while the primary crack in sample S2 was diffuse, and considerable deformation zone was distributed widely around the primary crack, as shown in Fig. 2(c–d). The area ahead of the crack tip was examined by EBSD (Fig. 2e–f). The strain distribution was analyzed by the local misorientation method of grain average misorientation (GAM) [12,13]. Strain was severely concentrated in the grains ahead of the crack tip in sample S1 (Fig. 2e). On the contrast, the grains ahead of the crack tip in sample S2 were less strained, and the strain concentrated at grain boundaries (Fig. 2f). The grains were classified into three groups according to the internal misorientation (θ), as shown in Fig. 2(e–f). Heavily deformed grains (θ greater than 3°) was observed at the crack tip in S1, corresponding to the strain concentrated grains, while there were almost no heavily deformed grains

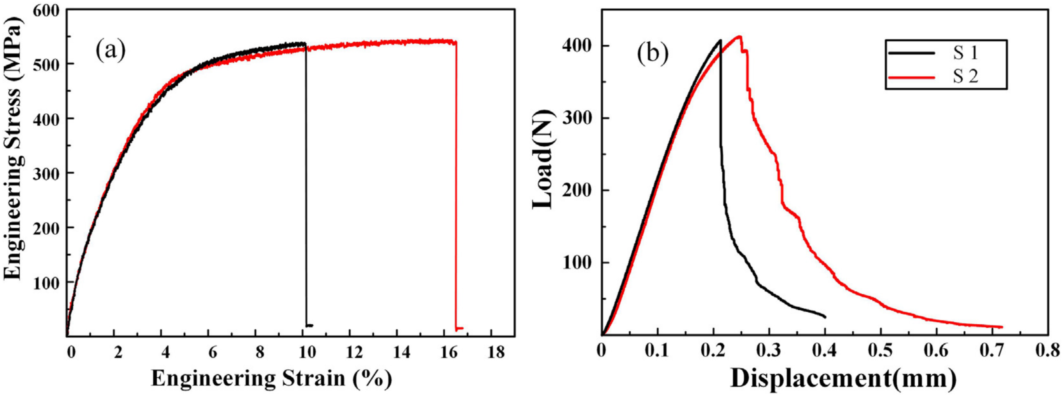

Fig. 1. (a) Tensile stress-strain curves; (b) load – indenter displacement curves of sample S1 and S2 by three-point bend testing.

Table 1
Typical mechanical properties including yield strength ($\sigma_{0.2}$), tensile strength (σ_b), total elongation (ε), linear-elastic plane-strain fracture toughness (K_I); elastic-plastic plane-strain fracture toughness (K_J); work of fracture (γ_{wof}).

Sample	$\sigma_{0.2}$ (MPa)	σ_b (MPa)	ε (%)	K_I ($MPa \cdot m^{1/2}$)	K_J ($MPa \cdot m^{1/2}$)	γ_{wof} (J/mm^2)
S1	310 ± 3	540 ± 3	10.4 ± 0.8	39.2 ± 0.3	71.3 ± 0.5	11.2 ± 0.5
S2	313 ± 5	545 ± 3	16.7 ± 1.2	39.1 ± 0.2	81.5 ± 0.5	17.5 ± 0.3

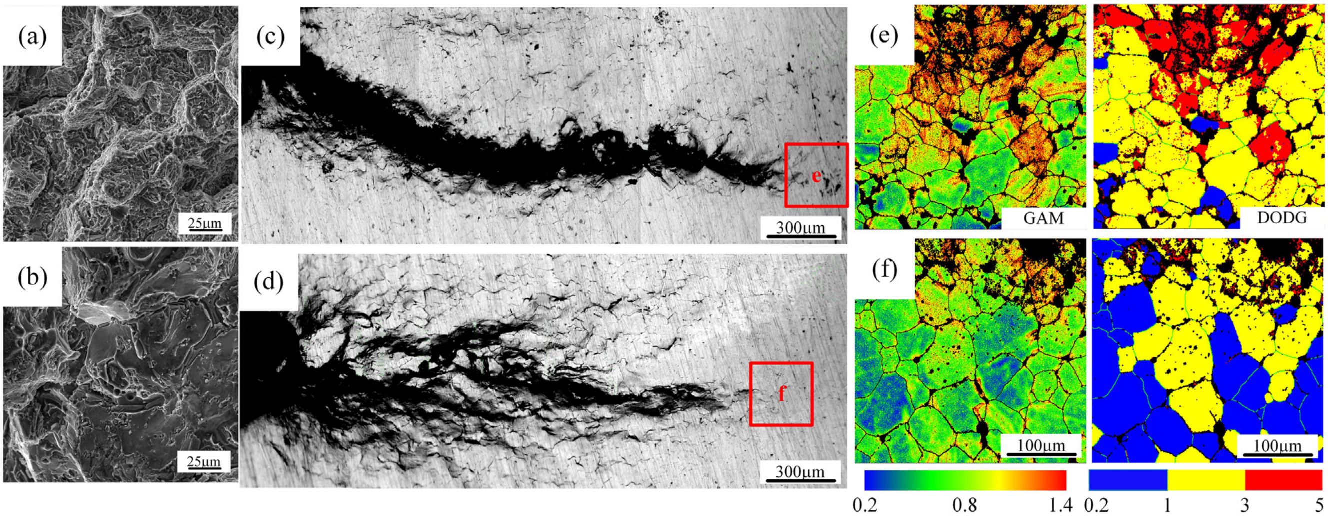

Fig. 2. Fracture surface morphology of sample S1 (a) and S2 (b) after tension testing; macro-cracks of sample S1 (c) and S2 (d) as ceased at the displacement = 0.4 mm in Fig. 2b; the tip of main crack and the corresponding EBSD analysis of sample S1 (e) and S2 (f).